


SCIENTIFIC ARTICLE

Upregulation of cGMP-dependent Protein Kinase (PRKG1) in the Development of Adolescent Idiopathic Scoliosis

Cang-long Hou, MD[#], Bo Li, MD[#], Ya-jun Cheng, MD[#], Ming Li, MD, Zong-de Yang, MD 

Department of spine surgery, Shanghai Changhai Hospital, Shanghai, China

Objective: To explore the molecular regulatory mechanisms underlying fibroblast differentiation and dysfunction in the development of adolescent idiopathic scoliosis (AIS) in an effort to identify candidate therapeutic targets for AIS.

Methods: The GSE110359 dataset, obtained from the bone marrow stromal cells of 12 AIS patients and five healthy controls, was retrieved from the GEO database. The data were preprocessed and differentially expressed genes (DEGs) were identified. KEGG pathway and Gene Ontology (GO)-Biological Process (BP) enrichment analyses were performed to identify the function of the DEGs. A protein–protein interaction (PPI) and a microRNA-transcription factor (TF)-target co-regulatory network were constructed to identify hub genes in the development of AIS. In addition, hub DEGs were evaluated by quantitative PCR (qPCR) and immunohistochemical staining.

Results: A total of 188 DEGs including 100 up-regulated and 88 down-regulated genes were obtained. The up-regulated DEGs were related to “p53 signaling pathway”, “FoxO signaling pathway”, and “cGMP-PKG signaling pathway” terms, while the down-regulated DEGs were significantly enriched in seven terms including “protein processing in endoplasmic reticulum”. The key up-regulated genes, *PRKG1*, *CCNG2*, and *KAT2B*, and the key down-regulated genes, *MAP2K1* and *DUSP6*, were identified by the PPI and miRNA-TF-Target regulatory network analyses. mRNA expression patterns for *PRKG1*, *DUSP6*, and *KAT2B* were successfully verified by qPCR. In addition, *PRKG1* protein levels were found to be elevated during the immunohistochemical analysis.

Conclusion: Increased expression of *PRKG1* in AIS patients might be an attractive therapeutic target for AIS. However, further gain or loss-of-function studies should be conducted.

Key words: Adolescent idiopathic scoliosis; cGMP-PKG signaling pathway; Differentially expressed genes; *PRKG1*

ABBREVIATION

AIS	adolescent idiopathic scoliosis
DEGs	differentially expressed genes
GO	Gene Ontology
BP	Biological Process

PPI	protein–protein interaction
TF	transcription factor
qPCR	quantitative PCR
PI3K	phosphoinositide 3-kinase
MSC	marrow stromal cells
GEO	Gene Expression Omnibus

Address for correspondence Zong-de Yang and Ming Li, Department of spine surgery, Shanghai Changhai Hospital, No.168, Changhai Road, Yangpu district, Shanghai, China 200433 Tel: +86-21-31166666; Email: yangzongde1969@aliyun.com (Yang) and limingch@21cn.com (Li)

[#]These authors contributed equally to this manuscript.

Authorship declaration We declared that all authors listed meet the authorship criteria according to the latest guidelines of the International Committee of Medical Journal Editors, and that all authors are in agreement with the manuscript.

Acknowledgements The authors would like to thank the editor for editing the manuscript.

Disclosure statement No benefits in any form had been received from a commercial party related to this article. The authors declared that there were no conflicts of interest.

Received 26 September 2019; accepted 15 April 2020

ORA	Overrepresentation Enrichment Analysis
qRT-PCR	Quantitative Reverse Transcription PCR
SD	standard deviation
PRKG1	protein kinase cGMP-dependent 1

Introduction

Adolescent idiopathic scoliosis (AIS) is the most common structural spinal deformity when the deformity exceeds 10 degrees¹. It affects approximately 2% to 4% of adolescents between 10 and 18 years of age^{1, 2}. Scoliosis surgery has a high rate of complication making it high-risk and expensive, which can impose a heavy economic burden on families and society. Therefore, understanding the molecular mechanism underlying AIS development is of vital importance and could help develop novel medical interventions.

Currently, the molecular mechanism of AIS has not been determined. It is believed that the occurrence and development of AIS involve multiple cell types and genes. Studies suggest that joint laxity is associated with AIS³, and the incidence of AIS in ballet dancers, who have a higher rate of hypermobility(70%), is significantly higher than that of non-dancers of the same age⁴. The distribution of collagen in adolescents with AIS is different from that of normal subjects⁵. In addition, connective tissue abnormalities including Marfan syndrome and Ehlers-Danlos syndrome are often associated with a higher incidence of spinal deformity^{6, 7}. These studies suggest that the pathogenesis of AIS may be closely related to collagen abnormalities. Collagen formation is mainly achieved by fibroblasts producing collagen-I, α -SMA, and fibronectin. Haller *et al.* found that variants in musculoskeletal collagen genes were significantly enriched in AIS compared to controls. They revealed that the fibrillar collagen gene *COL11A2* was highly associated with AIS⁸. In addition, many studies have suggested that TGF- β /Smad4 signaling, MMP-1, 2, 9, 13, Ras-MAPK signaling, and phosphoinositide 3-kinase (PI3K)-Akt

eNOS-NO signaling are the main regulators of collagen synthesis and degradation⁹⁻¹².

Fibroblasts were differentiated from bone marrow stromal cells (MSC). The role of fibroblast differentiation and dysfunction in the pathogenesis of scoliosis has received extensive attention. For example, several genes including TGF- β 1 and MMP3 were differentially expressed in the dense connective tissues of patients with AIS and could participate in the development of scoliosis^{13, 14}. However, current research on the role of fibroblast differentiation and dysfunction in the development of scoliosis remains unclear; this prevents them from being used as targets for clinical intervention.

Microarray-based studies have been widely conducted to investigate the molecular mechanism of AIS development. For example, Fendri *et al.* identified 145 differentially expressed genes (DEGs) between AIS patients and healthy control, including *FAM101A*, *ZIC2*, *PITX1*, and *COMP*¹⁵. This study aimed to: (i) explore the molecular regulatory mechanisms underlying fibroblast differentiation and dysfunction in the development of AIS; and (ii) identify candidate therapeutic targets for AIS. DEGs involved in collagen-related biological processes could be used as candidate therapeutic targets for the treatment of AIS in the future.

Methods

Microarray Data

In this study, we systematically screened DEGs in fibroblasts from normal and AIS patients, and explore the molecular mechanism of AIS pathogenesis using bioinformatic analyses (Fig. 1). The GSE110359 dataset was downloaded from the NCBI GEO database (Gene Expression Omnibus, <http://www.ncbi.nlm.nih.gov/geo/>)^{16, 17}(species: *Homo sapiens*). The data were obtained from MSCs from 12 AIS patients and five healthy controls. All subjects were less than 18 years of age. This data was generated on a GPL17586[HTA-2_0]

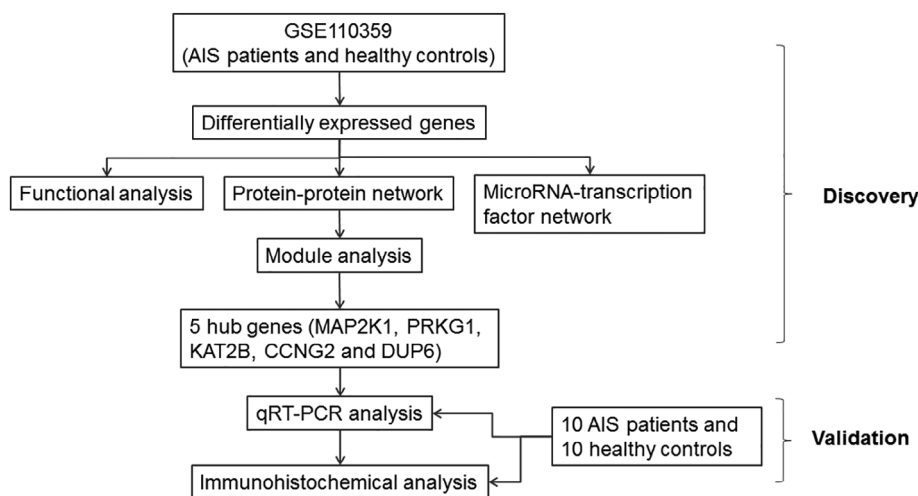


Fig 1 Schematic representation of the study design

platform using the Affymetrix Human Transcriptome Array 2.0 [transcript (gene) version].

Data Preprocessing and DEG Screening

The original CEL data were preprocessed and normalized using the Oligo program in R (version 1.36.1, <http://bioconductor.org/packages/release/bioc/html/oligo.html>). The probe was annotated in the platform annotation file and was used to remove probes that did not match the Gene symbol; for different probes that mapped to the same gene, the mean value for these probes was taken as the final expression value of the gene.

Differential expression analysis was conducted using the classical Bayesian method from the limma package (Version 3.10.3, <http://www.bioconductor.org/packages/2.9/bioc/html/limma.html>). Genes with a *P* value < 0.01 were identified as DEGs.

Enrichment Analysis of DEGs

DAVID¹⁸ (Version 6.8, <https://david-d.ncicrf.gov/>) was used to perform KEGG pathway, Gene Ontology (GO)-Biological Process (BP)¹⁹ enrichment analysis for upregulated and downregulated genes. The functional terms with enriched gene counts ≥ 2 and *P* values < 0.05 were considered significant.

Protein-Protein Interaction (PPI) Network and Module Analysis

The interactions between the proteins encoded by the DEGs were analyzed using the STRING (Version: 10.0, <http://www.string-db.org/>) database²⁰. The DEGs acted as the input gene set and the species was set as human. To obtain the highest number of interactions, the PPI score was set to 0.15 (low confidence). The PPI network was built using Cytoscape (version: 3.2.0, <http://www.cytoscape.org/>).

Proteins in the same module of the PPI network often have the same or similar functions. We used Cytoscape's MCODE²¹ (Version 1.4.2, <http://apps.cytoscape.org/apps/MCODE>) plugin to identify the most significant clustering

modules in the PPI network. The threshold value was a score > 5. KEGG pathway enrichment analysis of the genes in significant clustering modules was then performed.

Transcription Factor (TF)-miRNA-target Co-regulatory Network Analysis

The miRNA-target and TF-target enrichment prediction was performed using the Overrepresentation Enrichment Analysis (ORA) enrichment method from the WEB-based Gene Set Analysis Toolkit (Web Gestalt, <http://www.webgestalt.org/>)²². Only genes from significant modules were used for this analysis. The thresholds were set at a count ≥ 2 and *P* value < 0.05. The TF-target gene regulatory network and the miRNA-target gene regulatory network were combined to obtain them iRNA-TF-Target regulatory network.

Quantitative Reverse Transcription PCR (qRT-PCR)

Ten female AIS patients (mean age = 16.3) and 10 female subjects with vertebral fractures or lumbar disc herniation (mean age = 16.5) were enrolled in this study, and gave informed consent. Total RNA was extracted by TRIzol Reagent (TaKaRa, Dalian, China) from the ligament tissues of AIS patients and healthy subjects (*n* = 3 for each) as per the commercial protocol. Total RNA was reverse transcribed to cDNA using prime Script RT Master MIX (TaKaRa) and expression levels for *MAP2K1*, *PRKG1*, *KAT2B*, *DUSP6*, and *CCNG2* were detected with a Power SYBR Green PCR Master (Thermo Fisher) on an ABI 7500 (Applied Biosystems, Carlsbad, CA, USA). The relevant primer sequences can be found in Table 1. *GAPDH* was used as the housekeeping gene.

Immunohistochemical Localization of DEG-Encoded Proteins

Immunohistochemical analysis was performed as described previously²³. Briefly, ligament tissues were embedded and cut into 8 μ m thick frozen sections. Antigen recovery was performed by incubating the sections in 0.01 M citric acid buffer and the activity of endogenous peroxidases were blocked with 3% hydrogen peroxide for 15 min, followed by incubation with 10% goat serum for 1 h at 37°C to block non-specific binding reactions. The sections were incubated with a primary antibody against PRKG1 (1:100, Cat.no.: ab38007, Abcam) at 4°C overnight. We then added the goat anti-Rabbit IgG-HRP (H + L, 1: 400, Jackson ImmunoResearch, Cat.no.: 111-035-003). Sections were developed in diaminobenzidine solution for 1 min and counterstained with hematoxylin for 30 s, dehydrated, and sealed with neutral gum.

Statistical Analysis

Data were expressed as mean \pm standard deviation (SD). Experiments were conducted in triplicate. Gene expression differences detected by qRT-PCR between the two groups were compared using the Student's *t*-test in GraphPad prism

TABLE 1 The forward and reverse primers of genes and GAPDH normalizer for RT-PCR

Primer	Direction	Sequence (5'-3')
MAP2K1	Forward	CAATGGCGGTGTGGTGTTTC
	Reverse	GATTGCGGGTTTGATCTCCAG
PRKG1	Forward	GACAACGATGAACCACCAC
	Reverse	GCTTTGCTTCAGGACCAC
DUSP6	Forward	GAAATGGCGATCAGCAAGACG
	Reverse	CGACGACTCGTATAGCTCCTG
KAT2B	Forward	CGAATCGCCGTGAAGAAAGC
	Reverse	CTTGCAGCGGAGTACTACT
CCNG2	Forward	TAGCAGGACAGTGGATA
	Reverse	AATACTTGGGCAATAGGA
GAPDH	Forward	TGACAACCTTTGGTATCGTGAAGG
	Reverse	AGGCAGGGATGATGTTCTGGAGAG

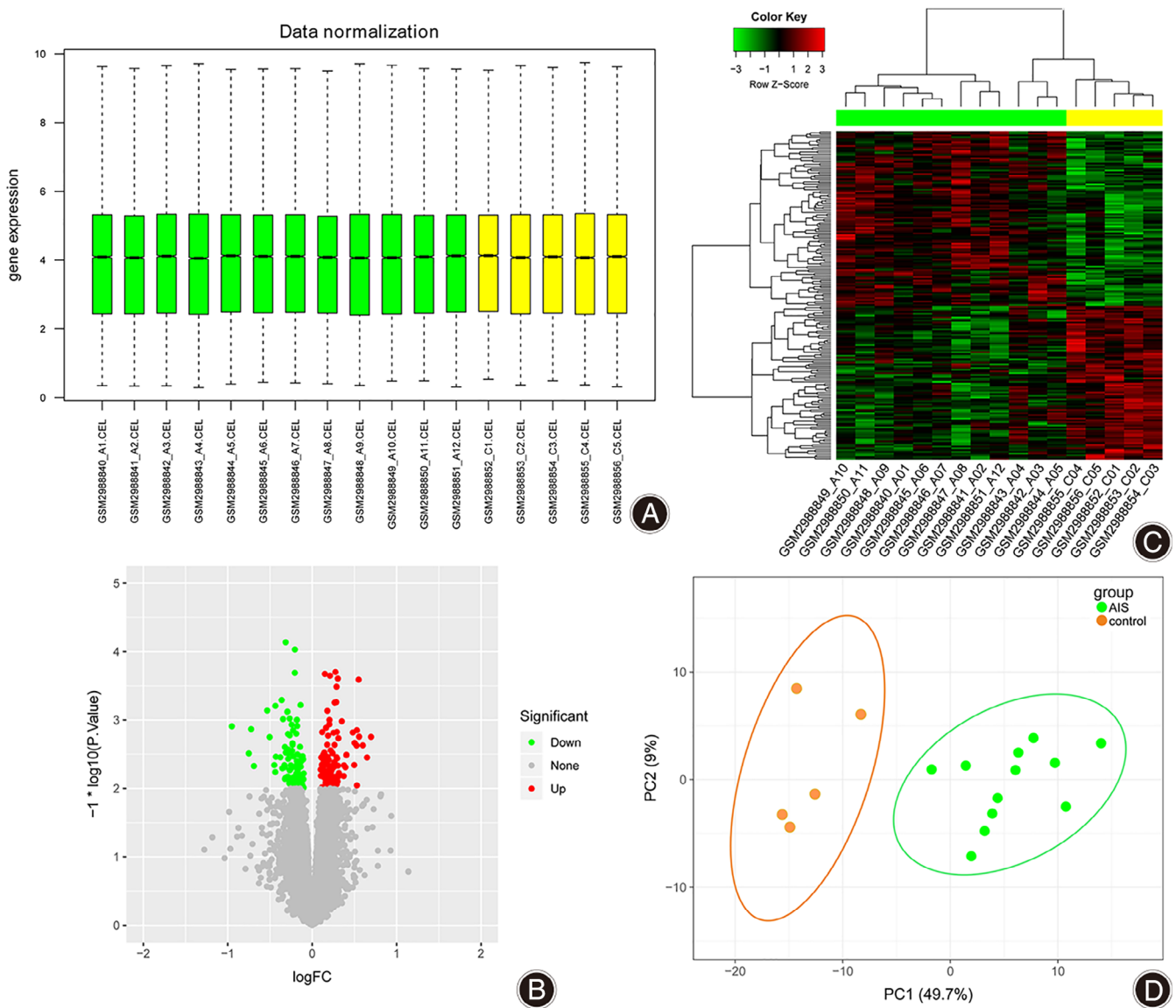


Fig 2 Box diagram after data preprocessing (A), volcano plot (B) heatmap diagram (C), and principal component analysis (PCA) plots (D) of gene expression profiles. Green are the AIS samples, and yellow are the control samples

5.0 (GraphPad Software Inc., San Diego, CA, USA). P values < 0.05 were regarded as statistically significant.

Results

Differential Expression Analysis

The distribution of the normalized expression values are represented in Fig. 2A and show the median values on the same horizontal line. A total of 188 DEGs with P value < 0.01 were identified. Of these, 100 were up-regulated and 88 were down-regulated (Fig. 2B and Table S1). The gene expression heatmap (Fig. 2C) and PCA plots (Fig. 2D) showed that

DEGs can be clearly distinguished in the disease samples when compared to the control.

DEG Functional Enrichment Results

The KEGG pathway enrichment analysis showed that up-regulated DEGs were significantly enriched in three pathways, including “p53 signaling pathway” ($n = 3$; $P = 3.04 \times 10^{-3}$), “FoxO signaling pathway” ($n = 3$; $P = 1.84 \times 10^{-2}$), and “cGMP-PKG signaling pathway” ($n = 3$; $P = 3.64 \times 10^{-2}$). The down-regulated DEGs were significantly enriched into seven pathways, including “Protein processing in endoplasmic reticulum” ($n = 4$;

TABLE 2 KEGG pathway and Gene Ontology (GO)-Biological Process (BP) analysis results of differentially expressed genes (DEGs)

	ID	Name	Count	P Value	Gene
Up-regulated genes					
Pathway	hsa04115	p53 signaling pathway	3	3.04E-03	DDB2;STEAP3;CCNG2
	hsa04068	FoxO signaling pathway	3	1.84E-02	FBXO32;RBL2;CCNG2
	hsa04022	cGMP-PKG signaling pathway	3	3.64E-02	GTF2I;PRKG1;PDE5A
GO-BP	GO:0006357	regulation of transcription from RNA polymerase II promoter	8	4.06E-03	CAMTA2, TSHZ1, ANKRA2, RBL2, GTF2I, TFDP2, VEZF1, BRD8
	GO:0006633	fatty acid biosynthetic process	3	2.37E-02	ELOVL4, FAXDC2, CBR4
	GO:0006091	generation of precursor metabolites and energy	3	2.46E-02	FECH, SLC25A27, DHTKD1
	GO:0007264	small GTPase mediated signal transduction	5	2.65E-02	PLD2, RASL11A, ARL17A, RALBP1, DOCK11
	GO:0007165	signal transduction	11	3.88E-02	RAP2B, RALBP1, GTF2I, PPP2R5D, PKIG, PDE5A, MCC, PRKG1, BRD8, DAPK1, DTNA
Down-regulated genes					
Pathway	hsa04141	Protein processing in endoplasmic reticulum	4	2.78E-03	ERO1A;STT3A;DERL1;TXNDC5
	hsa05020	Prion diseases	2	7.98E-03	LAMC1;MAP2K1
	hsa05110	Vibrio cholerae infection	2	1.58E-02	KDEL2;ERO1A
	hsa00510	N-Glycan biosynthesis	2	1.64E-02	STT3A;MGAT5
	hsa00590	Arachidonic acid metabolism	2	2.20E-02	PTGS1;CBR1
	hsa04610	Complement and coagulation cascades	2	3.24E-02	A2M;MBL2
	hsa05222	Small cell lung cancer	2	4.25E-02	LAMC1;TRAF3
GO-BP	GO:0006457	protein folding	4	2.65E-02	GRPEL1, ERO1A, TXNDC5, PDIA6
	GO:0034976	response to endoplasmic reticulum stress	3	2.95E-02	ERO1A, TXNDC5, PDIA6
	GO:0022617	extracellular matrix disassembly	3	3.02E-02	A2M, LAMC1, CTSG
	GO:0045454	cell redox homeostasis	3	3.10E-02	ERO1A, TXNDC5, PDIA6
	GO:0019371	cyclooxygenase pathway	2	3.52E-02	CBR1, PTGS1
	GO:0034975	protein folding in endoplasmic reticulum	2	4.55E-02	ERO1A, EMC1

$P = 2.78 \times 10^{-3}$) and “Complement and coagulation cascades” ($n = 2$; $P = 3.25 \times 10^{-2}$) (Table 2).

The GO-BP enrichment analysis revealed that the up-regulated DEGs were significantly enriched in five GO-BP terms, and the down-regulated DEGs were significantly enriched in six GO-BP terms (Table 2).

The PPI Network and Sub-Network Modules

To investigate the associations between the DEGs, we built a PPI network. As shown in Fig. 3A, the PPI network included 70 upregulated genes, 58 downregulated genes, and 483 pairs of interactions. Topological property of each node is displayed in Table S2. A total of 14 genes had a degree that was equal or larger than 20, including *RAP2B* (Upregulated gene, degree = 32), *KAT2B* (Upregulated gene, degree = 27), *PRKG1* (Upregulated gene, degree = 26), *PDIA6* (Downregulated gene, degree = 25), *ARL17A* (Upregulated gene, degree = 25), and *ANKRA2* (Upregulated gene, degree = 25). Since this network was too large and complex for more detailed analysis, we created a further mined sub-network of modules. As a result, we created a sub-network module (score = 6.471) which contained 18 nodes and 55 interaction pairs (Fig. 3B). The important upregulated (*PRKG1*, *CCNG2*, *KAT2B*, and *RBL2*) and down-regulated (*MAP2K1* and *DUSP6*) genes were included in this module. KEGG pathway analysis was performed on the genes in the significant clustering modules, and a total of nine KEGG pathway terms were shown to be enriched, including “FoxO signaling pathway” (*MAP2K1*, *RBL2*, and *CCNG2*), “vascular smooth

muscle contraction” (*PRKG1* and *MAP2K1*), “thyroid hormone signaling pathway” (*MAP2K1* and *KAT2B*), “cGMP-PKG signaling pathway” (*PRKG1* and *MAP2K1*), “MAPK signaling pathway” (*DUSP6* and *MAP2K1*), and “PI3K-Akt signaling pathway” (*MAP2K1* and *RBL2*) (Table 3).

The miRNA-TF-target Regulatory Network

A total of 21 miRNAs and six TFs that target the genes in the significant modules were predicted using WebGestalt, and a miRNA-TF-Target regulatory network involving these 21 miRNAs, six TFs, three down-regulated DEGs, and 10 up-regulated DEGs was then constructed (Fig. 4). For the DEGs related to vascular smooth muscle contraction, *PRKG1* was targeted by miR-199a, miR-522 and *OCT1/MAP2K1* were targeted by miR-324-3p, miR-181a, miR-181b, miR-181c, miR-181d, miR-330, miR-199a, and *PAX4*. Other upregulated genes including *TNRC6*, *HECA*, *DOCK1*, *RASL11A*, *KLHL24*, *CCNG2*, *KAT2B*, and *RBL2*, and the down-regulated genes *KLF10* and *DUSP6* were also included in the network.

qRT-PCR and Immunohistochemical Analysis

Five critical genes, *MAP2K1*, *PRKG1*, *DUSP6*, *KAT2B*, and *CCNG2* were selected for qRT-PCR validation. As shown in Fig. 5, qRT-PCR showed that the mRNA expression levels of *PRKG1*, *DUSP6*, and *KAT2B* were the same as those predicted by the DEG analysis from the microarray data ($P < 0.05$). Since *PRKG1* is involved in “Vascular smooth muscle contraction”, we further characterized its expression

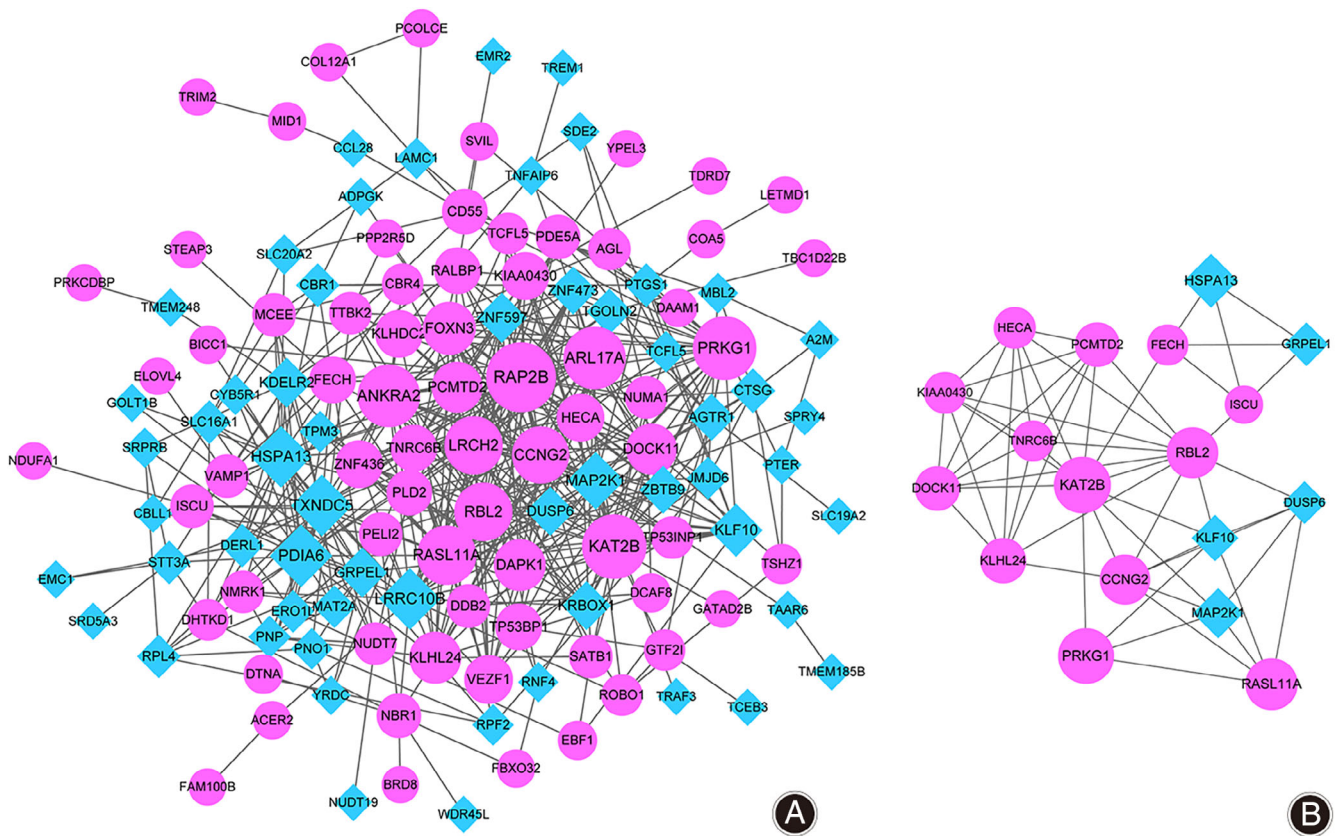


Fig 3 The protein-protein interaction (PPI) network of differentially expressed genes in AIS (A). This significant clustering modules of the PPI network (B). The circle nodes indicate the up-regulated genes, and the diamond nodes represent the down-regulated genes.

TABLE 3 KEGG pathway enriched by differentially expressed genes (DEGs) in the sub-network module

ID	Name	Count	P Value	Genes
hsa04068	FoxO signaling pathway	3	2.17E-04	MAP2K1;RBL2;CCNG2
hsa04730	Long-term depression	2	1.53E-03	PRKG1;MAP2K1
hsa04540	Gap junction	2	3.45E-03	PRKG1;MAP2K1
hsa04270	Vascular smooth muscle contraction	2	5.98E-03	PRKG1;MAP2K1
hsa04919	Thyroid hormone signaling pathway	2	6.09E-03	MAP2K1;KAT2B
hsa04022	cGMP-PKG signaling pathway	2	1.16E-02	PRKG1;MAP2K1
hsa05203	Viral carcinogenesis	2	1.50E-02	RBL2;KAT2B
hsa04010	MAPK signaling pathway	2	2.53E-02	DUSP6;MAP2K1
hsa04151	PI3K-Akt signaling pathway	2	4.45E-02	MAP2K1;RBL2

by immunohistochemistry. The results showed that the expression levels of PRKG1 protein in the AIS group were also elevated when compared with the control group (Fig. 6).

Discussion

AIS is the most common structural spinal deformity. However, its pathological mechanism is still largely unknown. In this study, we retrieved an AIS microarray

dataset and used it to investigate the potential molecular mediators of its pathological mechanism. As a result, we identified a total of 188 DEGs between AIS and control samples. Further analysis suggested that the “p53 signaling pathway”, “FoxO signaling pathway”, and “cGMP-PKG signaling pathway” were activated while “Protein processing in endoplasmic reticulum” and “Complement and coagulation cascades” pathways were suppressed in AIS patients. Five

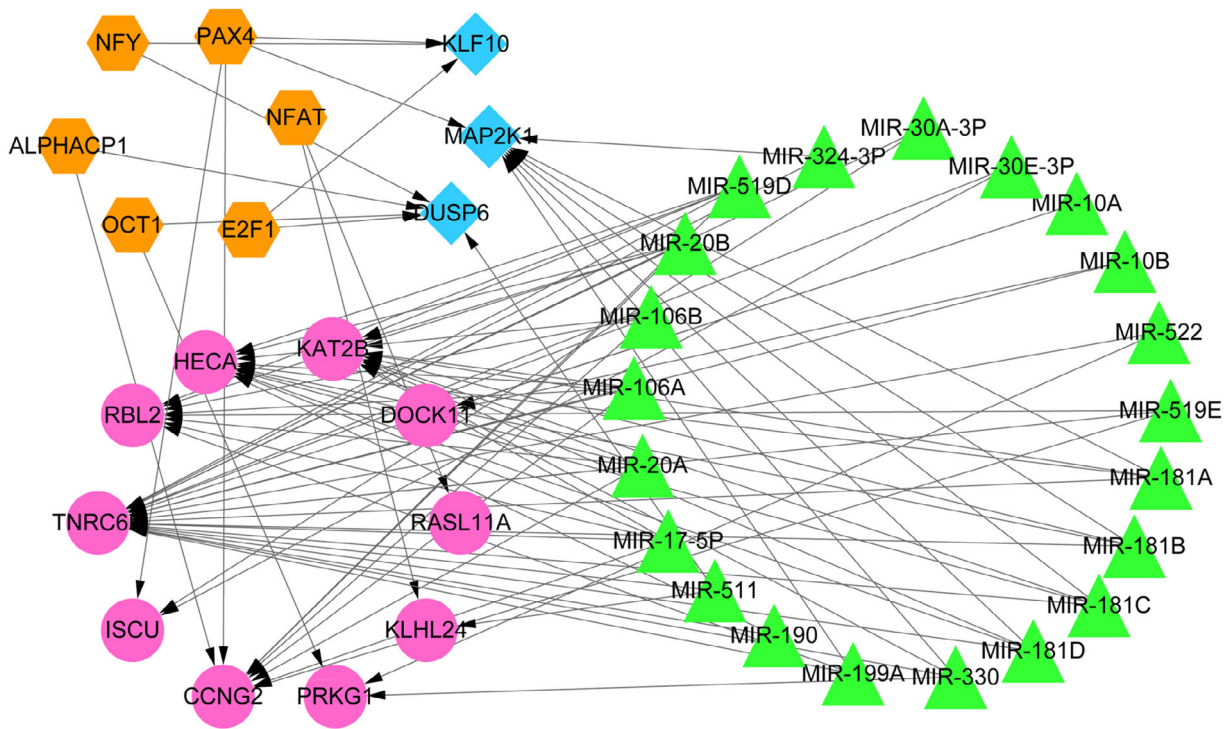


Fig 4 The microRNA-transcription factor-Target regulatory network. The triangle nodes are miRNAs, the hexagon nodes are transcription factors, and edges with an arrow indicate regulatory relationships.

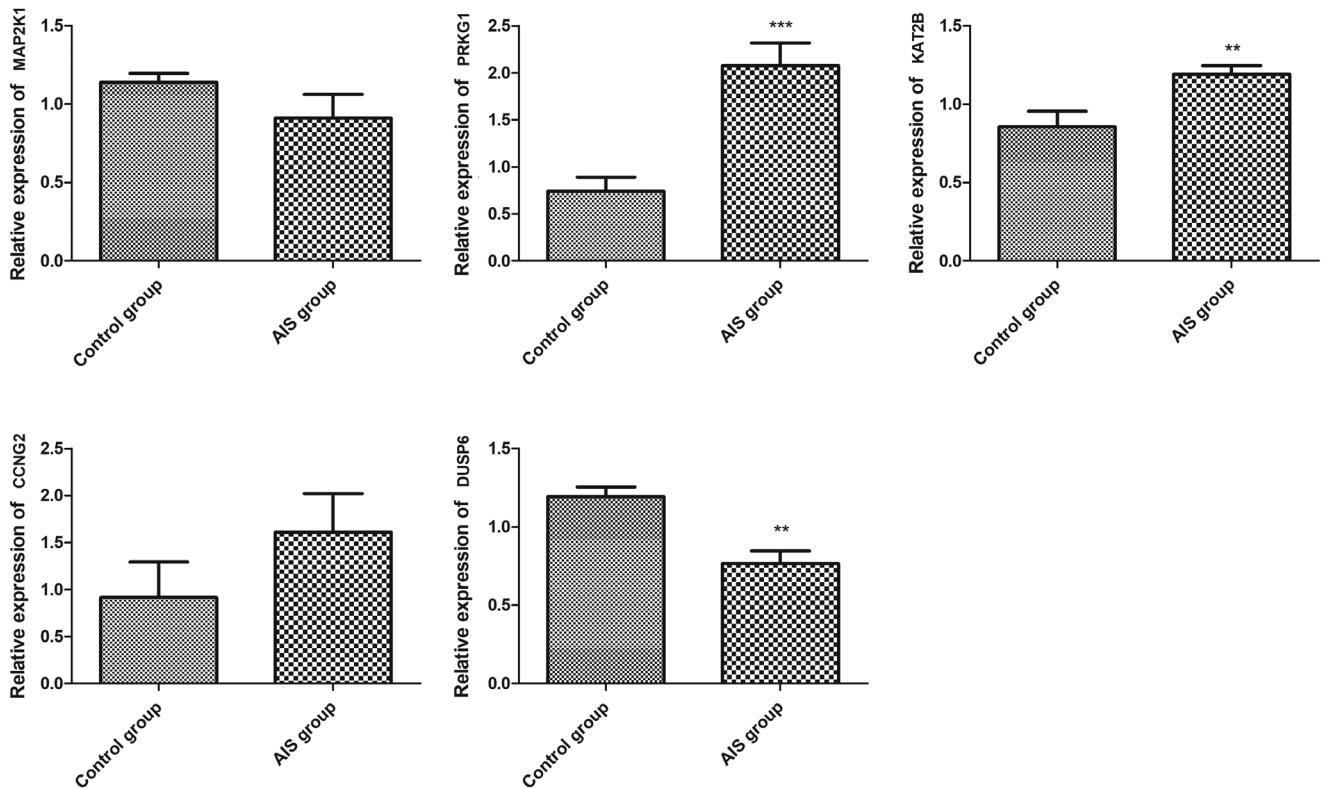


Fig 5 The qRT-PCR analysis of five crucial genes, including MAP2K1, PRKG1, KAT2B, CCNG2 and DUSP6. Data were expressed as mean ± standard deviation. Comparisons between groups were calculated by student's t test. *, $P < 0.05$; **, $P < 0.01$; ***, $P < 0.001$.

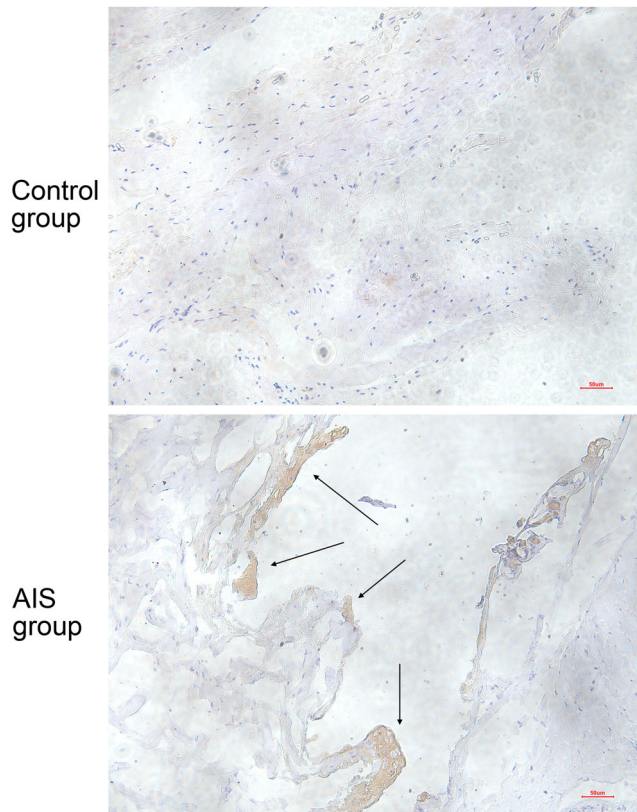


Fig 6 The protein expression of PRKG1 detected by immunohistochemical analysis ($\times 200$). The arrow indicates PRKG1 expression.

crucial nodes in the PPI and miRNA-TF-target networks were identified. These included *MAP2K1*, *PRKG1*, *DUSP6*, *KAT2B*, and *CCNG2* which were further verified using qRT-PCR and we were able to confirm the expression profiles of *PRKG1*, *DUSP6*, and *KAT2B*. In addition, immunohistochemical analysis was carried out to evaluate the protein expression of PRKG1 in AIS patients.

PRKG1 (protein kinase cGMP-dependent 1) was significantly enriched in “cGMP-PKG signaling”, “Gap junction”, and “Vascular smooth muscle contraction” and may be important in the complex pathological mechanisms of AIS. PRKG1 acts as key mediator of the nitric oxide/cGMP signaling pathway and is an important component in many signal transduction processes in diverse cell types. PRKG1 has been shown to be associated with RhoA activity and Akt signaling and was identified as a novel negative regulator of osteoblast differentiation in human skeletal (mesenchymal) stem cell²⁴. In our study, PRKG1 was shown to be upregulated at both the transcript and protein levels, and was linked to the following KEGG pathways “cGMP-PKG signaling”, “Long-term depression”, “Gap junction”, and “Vascular smooth muscle contraction”, as well as the GO-BP

term “signal transduction”. Hewitson *et al.* indicated that treatment with dipyridamole decreased fibroblast mitogenesis and collagen synthesis via the cGMP-PKG pathway.²⁵ Phosphodiesterase inhibitors, which increase cellular cGMP concentrations, induce the synthesis of collagen in keloid fibroblasts²⁶. Collagen-induced platelet secretion and aggregation is also mediated through cAMP and cGMP-independent signaling²⁷.

In addition, MAP2K1, which was shown to be down regulated in the expression study, interacts directly with PRKG1, and is involved in cGMP-PKG signaling, as well as MAPK and PI3K-Akt signaling. Mutant MAPK7-induced AIS has been linked to impaired osteogenesis²⁸. Previous study has indicated that p38 and MAPK play important roles in the production of collagen in fibroblasts²⁹. Moreover, the activation of MAPK signaling and the PI3K/Akt pathway promote fibroblast migration³⁰. The activation of PI3K/Akt pathway is associated with the normal regulation of MSC functions and has applications in tissue regeneration^{31, 32}. Degeneration of the intervertebral discs, which are primarily composed of water, aggrecan, and fibrillar collagens, could be prevented by the activation of the PI3K/Akt pathway as it increases extracellular matrix production, preventing apoptosis and oxidative damage, and facilitating cell proliferation³³. Therefore, MAP2K1 interactions with PRKG1 may indicate that PRKG1 is also an important candidate in the pathogenesis of AIS.

However, this study inevitably has some limitations. First, the sample size of this study is relatively small. Only 12 AIS patients and five healthy controls were analyzed from microarray study and key genes were validated in 10 AIS patients and 10 controls. Second, the molecular mechanism of PRKG1 in the development of AIS still needs further investigation. Therefore, further *in vitro* and *in vivo* studies should be conducted.

Conclusion

In conclusion, we identified a total of 188 DEGs following a comparison of expression data from AIS and healthy control samples. Further analysis suggested that the “p53 signaling pathway”, “FoxO signaling pathway”, and “cGMP-PKG signaling pathway” were activated, while “Protein processing in endoplasmic reticulum” and “Complement and coagulation cascades” pathways were suppressed in AIS patients. Increased expression of PRKG1 in AIS patients was confirmed by qRT-PCR and immunohistochemical staining, indicating that it may be an attractive therapeutic target for novel intervention strategies in the treatment of AIS. However, further gain and loss of function studies should be conducted to evaluate this hypothesis.

Supporting Information

Additional Supporting Information may be found in the online version of this article on the publisher’s web-site:

Table S1 The list of 188 differentially expressed genes.

Supporting Information

Additional Supporting Information may be found in the online version of this article on the publisher's web-site:

Table S2 Topological property of each node of the protein–protein interaction network.

REFERENCES

- Weinstein SL. The natural history of adolescent idiopathic scoliosis. *J Pediatr Orthop*, 2019, 39: S44–S46.
- Theroux J, Stomski N, Hodgetts CJ, et al. Prevalence of low back pain in adolescents with idiopathic scoliosis: a systematic review. *Chiropr Man Therap*, 2017, 25: 10.
- Binns M. Joint laxity in idiopathic adolescent scoliosis. *J Bone Joint Surg Br*, 1988, 70: 420–422.
- Zaina F, Donzelli S, Romano M, Negrini S. Prevalence and predictors of adolescent idiopathic scoliosis in adolescent ballet dancers. *Arch Phys Med Rehabil*, 2015, 96: 1181.
- Roberts S, Menage J, Eisenstein SM. The cartilage end-plate and intervertebral disc in scoliosis: calcification and other sequelae. *J Orthop Res*, 1993, 11: 747–757.
- Akpinar S, Gogus A, Talu U, Hamzaoglu A, Dikici F. Surgical management of the spinal deformity in Ehlers-Danlos syndrome type VI. *Eur Spine J*, 2003, 12: 135–140.
- Gjolaj JP, Sponseller PD, Shah SA, et al. Spinal deformity correction in Marfan syndrome versus adolescent idiopathic scoliosis: learning from the differences. *Spine*, 2012, 37: 1558–1565.
- Haller G, Alvarado D, McCall K, et al. A polygenic burden of rare variants across extracellular matrix genes among individuals with adolescent idiopathic scoliosis. *Hum Mol Genet*, 2016, 25: 202–209.
- Wang H, Mehta JL, Chen K, Zhang X, Li D. Human urotensin II modulates collagen synthesis and the expression of MMP-1 in human endothelial cells. *J Cardiovasc Pharmacol*, 2004, 44: 577–581.
- Zhai YK, Guo XY, Ge BF, et al. Icarin stimulates the osteogenic differentiation of rat bone marrow stromal cells via activating the PI3K-AKT-eNOS-NO-cGMP-PKG. *Bone*, 2014, 66: 189–198.
- Daniels JT, Limb GA, Saarialho-Kere U, Murphy G, Khaw PT. Human corneal epithelial cells require MMP-1 for HGF-mediated migration on collagen I. *Invest Ophthalmol Vis Sci*, 2003, 44: 1048–1055.
- Hu HH, Chen DQ, Wang YN, et al. New insights into TGF-beta/Smad signaling in tissue fibrosis. *Chem Biol Interact*, 2018, 292: 76–83.
- Nowak R, Kwiecien M, Tkacz M, Mazurek U. Transforming growth factor-beta (TGF-beta) signaling in paravertebral muscles in juvenile and adolescent idiopathic scoliosis. *Biomed Res Int*, 2014, 2014: 594287.
- Mónika M, Agnes C, Grózer ZB, et al. Association study of BMP4, IL6, leptin, MMP3, and MTNR1B gene promoter polymorphisms and adolescent idiopathic scoliosis. *Spine*, 2011, 36: E123–E130.
- Fendri K, Patten SA, Kaufman GN, et al. Microarray expression profiling identifies genes with altered expression in adolescent idiopathic scoliosis. *Eur Spine J*, 2013, 22: 1300–1311.
- Barrett T, Suzek TO, Troup DB, et al. NCBI GEO: mining millions of expression profiles—database and tools. *Nucleic Acids Res*, 2005, 33: D562–D566.
- Zhuang Q, Ye B, Hui S, et al. Long noncoding RNA IncAIS downregulation in mesenchymal stem cells is implicated in the pathogenesis of adolescent idiopathic scoliosis. *Cell Death Differ*, 2019, 26: 1700–1715.
- Huang DW, Sherman BT, Lempicki RA. Systematic and integrative analysis of large gene lists using DAVID bioinformatics resources. *Nat Protoc*, 2009, 4: 44–57.
- Ashburner M, Ball CA, Blake JA, et al. Gene ontology: tool for the unification of biology. *Nat Genet*, 2000, 25: 25–29.
- Szklarczyk D, Franceschini A, Wyder S, et al. STRING v10: protein-protein interaction networks, integrated over the tree of life. *Nucleic Acids Res*, 2015, 43: D447–D452.
- Bandettini WP, Kellman P, Mancini C, et al. MultiContrast delayed enhancement (MCOE) improves detection of subendocardial myocardial infarction by late gadolinium enhancement cardiovascular magnetic resonance: a clinical validation study. *J Cardiovasc Magn Reson*, 2012, 14: 83.
- Zhang B, Kirov S, Snoddy J. WebGestalt: an integrated system for exploring gene sets in various biological contexts. *Nucleic Acids Res*, 2005, 33: W741–W748.
- Ling ZQ, Guo W, Lu XX, et al. A Golgi-specific protein PAQR3 is closely associated with the progression, metastasis and prognosis of human gastric cancers. *Ann Oncol*, 2014, 25: 1363–1372.
- Boerth NJ, Dey NB, Cornwell TL, Lincoln TM. Cyclic GMP-dependent protein kinase regulates vascular smooth muscle cell phenotype. *J Vasc Res*, 1997, 34: 245–259.
- Hewitson TD, Tait MG, Kelynack KJ, Martic M, Becker GJ. Dipyridamole inhibits in vitro renal fibroblast proliferation and collagen synthesis. *J Lab Clin Med*, 2002, 140: 199–208.
- Margarucci L, Roest M, Preisinger C, et al. Collagen stimulation of platelets induces a rapid spatial response of cAMP and cGMP signaling scaffolds. *Mol Biosyst*, 2011, 7: 2311–2319.
- Li Z, Zhang G, Marjanovic JA, Ruan C, Du X. A platelet secretion pathway mediated by cGMP-dependent protein kinase. *J Biol Chem*, 2004, 279: 42469–42475.
- Zhou T, Chen C, Xu C, et al. Mutant MAPK7-induced idiopathic scoliosis is linked to impaired osteogenesis. *Cell Physiol Biochem*, 2018, 48: 880–890.
- Yu XY, Qiao SB, Guan HS, Liu SW, Meng XM. Effects of visfatin on proliferation and collagen synthesis in rat cardiac fibroblasts. *Horm Metab Res*, 2010, 42: 507–513.
- Clement DL, Mally S, Stock C, et al. PDGFRalpha signaling in the primary cilium regulates NHE1-dependent fibroblast migration via coordinated differential activity of MEK1/2-ERK1/2-p90RSK and AKT signaling pathways. *J Cell Sci*, 2013, 126: 953–965.
- Li W, Fan J, Chen M, et al. Mechanism of human dermal fibroblast migration driven by type I collagen and platelet-derived growth factor-BB. *Mol Biol Cell*, 2004, 15: 294–309.
- Macagno EO, Christensen J, Lee CL. Modeling the effect of wall movement on absorption in the intestine. *Am J Physiol*, 1982, 243: G541–G550.
- Ouyang ZH, Wang WJ, Yan YG, Wang B, Lv GH. The PI3K/Akt pathway: a critical player in intervertebral disc degeneration. *Oncotarget*, 2017, 8: 57870–57881.